LANGMUIR

pubs.acs.org/Langmuir Perspective

From Frustration to Order: Role of Fluid–Fluid Interfaces in Precision Assembly of Nanoparticles

Yilong Zhou, Şafak Çallıoğlu, and Gaurav Arya*

Cite This: *Langmuir* 2024, 40, 26800–26810 Read Online

ACCESS | Metrics & More | Article Recommendations

ABSTRACT: Fluid–fluid interfaces are an attractive platform for self-assembling nanoparticles into low-dimensional materials. In this Perspective, we review recent developments in the use of interfaces to direct the assembly of spherical and anisotropic nanoparticles into diverse and sophisticated architectures. We illustrate how nanoparticle clusters, strings, networks, superlattices, chiral lattices, and quasicrystals can be self-assembled by harnessing the frustration between interfacial and interparticle forces. We highlight the role of polymeric ligands attached to the surface of nanoparticles in modulating assembly behavior by directly altering particle–fluid and particle–particle interactions or by deforming at interfaces and junctions between particles. We conclude by providing a roadmap of key questions and opportunities in this exciting field of interfacial assembly.

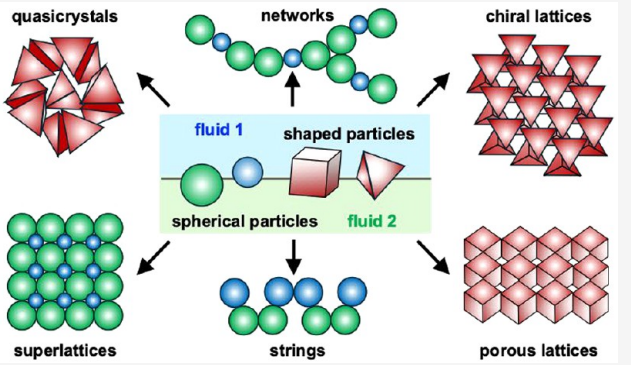

Downloaded via UNIV OF CALIFORNIA SAN DIEGO on January 30, 2025 at 19:38:06 (UTC).
See https://pubs.acs.org/sharingguidelines for options on how to legitimately share published articles.

INTRODUCTION

Self-assembly of nanoparticles (NPs) is a high-throughput, low-cost, and versatile strategy for fabricating nanostructured materials. NP assemblies can exhibit unique collective electronic, magnetic, and optical properties, owing to couplings between the excitons, magnetic dipoles, and plasmons of individual nanoparticles.[1] The large surface area coupled with the proximity of similar or distinct chemically active surfaces provided by NPs in assemblies can also lead to new or enhanced catalytic properties.[2] Furthermore, inorganic NPs introduced into polymers have been shown to improve their mechanical properties, especially when they self-assemble into percolating architectures.[3] Because of all these attributes, NP assemblies are finding potential applications in magnetoresistance devices,[4] surface-enhanced Raman spectroscopy,[5] optical metamaterials,[6] catalysis,[2] and polymer nanocomposites.[3]

Interfaces offer a powerful platform for self-assembly because of their ability to trap NPs and promote their assembly along the interface, enabling the formation of 2D or quasi-2D structures. Interfaces appear in various forms (fluid–fluid, fluid–solid, or solid–solid) and shapes (planar, curved, or bicontinuous). Planar fluid–fluid interfaces such as those formed between air and water, or oil and water, are particularly useful because they enable the formation of large-scale, free-floating assemblies at the interface, which could then be easily transferred onto a solid substrate, enabling facile integration with other materials and devices.[4,7] Additionally, the greater mobility of fluid-dispersed particles and their easier access to vacancies in the assembling structure from both fluid phases allow for rapid assembly with minimal structural defects.

In this Perspective, we review recent advances and outstanding problems in the use of fluid–fluid interfaces to self-assemble diverse NP assemblies. We will first discuss how even simple spherical NPs can assemble into complex anisotropic architectures at interfaces by harnessing the competition between interfacial and interparticle forces that appears during coassembly of multiple species of particles. Next, we discuss how fluid interfaces can be used to control the orientation of anisotropic NPs, enabling the formation of even more sophisticated assembly architectures. Third, we discuss the role of ligands, particularly long polymer chains tethered to NP surfaces, in introducing patchy attraction, steric repulsion, and multibody interactions between particles, which lead to the formation of intriguing emergent assemblies. We end by highlighting several open questions and challenges in the field of interfacial assembly. To keep the review focused, we will restrict our discussion to assembly cases driven by simple, short-ranged intermolecular or entropic forces between hard NPs or ligand-grafted NPs with hard cores. Although also

Received: August 23, 2024
Revised: November 27, 2024
Accepted: December 2, 2024
Published: December 12, 2024

ACS Publications © 2024 American Chemical Society

https://doi.org/10.1021/acs.langmuir.4c03321
Langmuir 2024, 40, 26800–26810

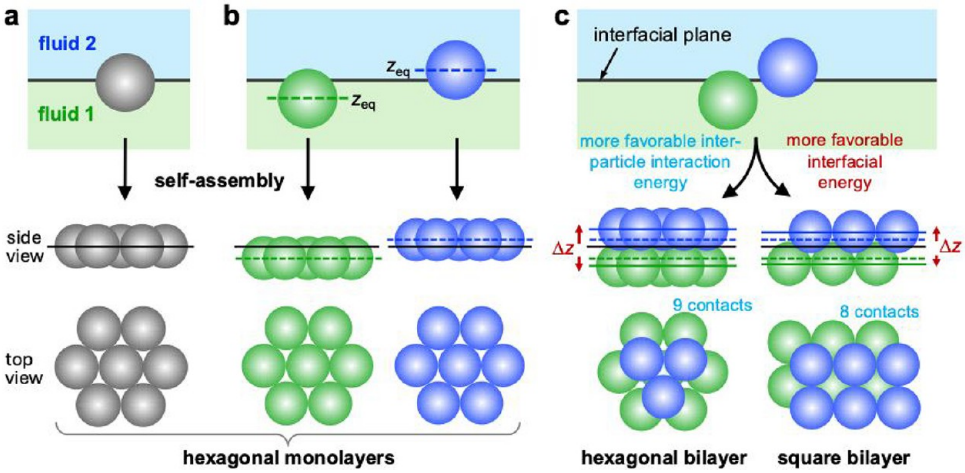

Figure 1. Interfacial assembly of spherical NPs. (a, b) Individual species of NPs self-assemble into hexagonal monolayers irrespective of whether the particles are impartial (panel (a)) or partial to a specific fluid of the interface (panel (b)). (c) In contrast, when two different species of NPs trapped at different planes z_{eq} (dashed green and blue lines) parallel to the interfacial plane (solid black line) are coassembled, a competition between interfacial forces and interparticle forces ensues. This results in frustrated assembly structures that best balance the number of favorable interparticle contacts they gain from assembly versus the interfacial energy particles lose by positioning themselves at a plane (solid green and blue lines) different from their preferred plane, as denoted by displacement Δz.

relevant to interfacial assembly, the behavior of soft, deformable particles (e.g., microgels)[8−11] and of particles interacting with more complex, long-range forces (e.g., capillary and electrostatic interactions)[12−17] will not be discussed, as these topics have been extensively reviewed in other review articles.

SPHERICAL NANOPARTICLES

Before discussing the assembly of spherical NPs, consider first the behavior of individual NPs at a fluid−fluid interface. If a particle exhibits equally favorable interactions with the two mutually incompatible fluids making up the interface, it will symmetrically position itself about the interfacial plane so that it can occlude the largest possible area (Figure 1a). However, NPs will generally show a preference for one fluid over the other. In such cases, the particle will move away from the interfacial plane toward the fluid it favors to minimize the free energy of the system (Figure 1b). Using a particle of radius R fully immersed in its favored fluid as reference, the free-energy change associated with bringing the particle to distance z from the interfacial plane is given by $\Delta F_1(z) = -A_0(z)\gamma + A_c(z)\Delta\gamma$, where γ is the surface tension between the two fluids and $\Delta\gamma > 0$ is the difference in the surface energy (per unit area) of the NP with the two fluids.[18−20] The first term in $\Delta F_1(z)$ describes the gain in free energy due to the particle occluding a circular area $A_0 = \pi(R^2 - z^2)$ of the interface, and the second term is the loss in free energy resulting from the particle's spherical cap of surface area, $A_c = 2\pi R(R + z)$, that is now forced to interact with the less-favored fluid. Here, we have ignored the contribution to the free-energy change from line tension given by $\tau L_0(z)$, where τ is the line tension and $L_0(z)$ is the perimeter of the particle-occluded area of the interface, as this term becomes negligible for sufficiently large NPs ($R \gg \tau/\gamma$).[14,21] Minimizing ΔF_1 with respect to z yields the equilibrium displacement of the NP from the interfacial plane, $z_{eq} = (\Delta\gamma/\gamma)R$, which grows linearly with the interaction difference $\Delta\gamma$.

Consider now multiple such NPs trapped at the interface. If the particles interact favorably with each other and are present at sufficiently high concentrations, they will self-assemble into a higher-order structure. Then, the net free-energy change for N interacting NPs can be written as

$$\Delta F_N = \sum_{i=1}^{N} \Delta F_1(z_i) + \sum_{i=1}^{N-1} \sum_{j=i+1}^{N} U_2(r_{ij})$$

where i is the particle index, r_{ij} is the distance between pairs of NPs, and U_2 is the effective pairwise potential describing their interaction. Minimizing ΔF_N should yield the optimal arrangement of NPs in the assembly; we assume here that entropy variations across the different NP assemblies are relatively small, compared with variations in their potential energy from interparticle interactions, which need to be strong enough in the first place to promote assembly. It turns out that both terms in ΔF_N can be simultaneously minimized for a single species of NPs trapped in 2D to yield a triangular lattice positioned at $z = z_{eq}$ (see Figures 1a and 1b). To achieve more distinctive assemblies, one then needs: (1) more than one species of NPs that interact differently with the two fluids so that they get trapped at distinct planes parallel to the interfacial plane, and (2) a gap between these trapping planes that is small enough to facilitate interparticle interactions across them (Figure 1c).[18,19] In such cases, it is *not* possible to achieve assemblies that can simultaneously minimize the interfacial and interparticle energy terms. Thus, a competition between the two types of interactions must ensue—one attempting to assemble individual species into separate monolayers and the other attempting to pack particles of all species into multilayered or 3D globular structures. This leads to "frustrated" assemblies with highly unique particle arrangements that go beyond conventional triangular monolayers or hexagonally ordered bilayers.

This concept has been experimentally implemented via the solvent-evaporation method to realize complex 2D assemblies. In this approach, an organic solvent (e.g., hexane or toluene) carrying well-dispersed NPs is injected onto the surface of a polar liquid (e.g., water or diethylene glycol). Slow evaporation of the solvent then promotes the formation of 2D or quasi-2D structures at the air−liquid interface, wherein both interparticle interactions and entropy (due to the confinement effects of

https://doi.org/10.1021/acs.langmuir.4c03321
Langmuir 2024, 40, 26800−26810

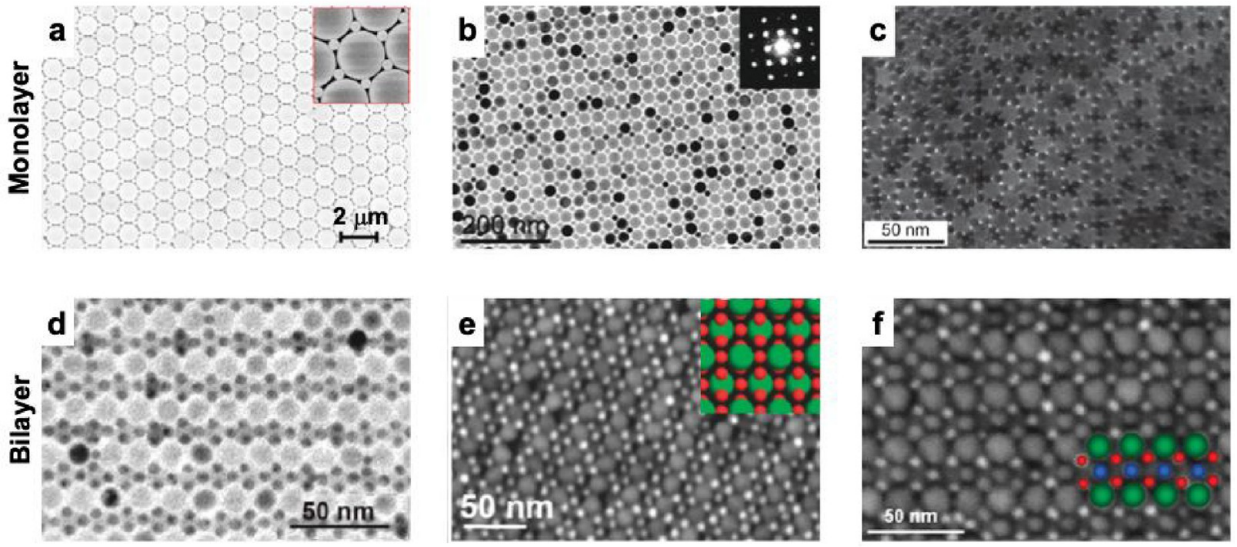

Figure 2. Mono and bilayer superlattices obtained from self-assembly of spherical NPs at a fluid−fluid interface. (a) AB_2-type triangular lattice of 200 and 1000 nm polystyrene NPs. (b) AB-type intertwined square lattice of 28.9 nm $NaFY_4$:Yb/Er and 13.4 nm Fe_3O_4 NPs. (c) Dodecagonal quasicrystals of 13.4 nm Fe_2O_3 and 5 nm Au NPs. (d) A_2B_3-type bilayer of 11.2 nm Fe_3O_4 and 6.4 nm Au NPs. (e) AB_3-type bilayer of 16.5 nm Fe_3O_4 and 6.0 nm FePt NPs. (f) ABC_2-type bilayers 16.5 nm Fe_3O_4, 7.0 nm Fe_3O_4, and 5.0 nm FePt NPs. [Panel (a) has been adapted with permission from ref 7. Copyright 2016, American Chemical Society, Washington, DC. Panels (b), (d), (e), and (f) have been adapted with permission from ref 23. Copyright 2011, American Chemical Society, Washington, DC. Panel (c) has been adapted with permission from ref 28. Copyright 2009, Springer Nature.]

evaporation) are expected to drive self-assembly. Subsequently, a substrate is placed beneath the floating structure and carefully lifted to the liquid interface to minimize alterations in the structure during its transfer onto the substrate for imaging.[4,22] In this manner, researchers have assembled simple triangular monolayers from a single species of spherical NPs,[5,6] as well as more complex assemblies such as AB_2-type triangular,[4,7,23,24] AB-type intertwined square,[2,23] AB_6- and AB_7-type hexagonal,[7] and ico-AB_{13}-type square monolayers[4] from two different-sized species of NPs (Figures 2a and 2b). These monolayers likely appear when $\Delta\gamma_1 \approx \Delta\gamma_2$, that is, when both species have similar preference for the two fluids, so they prefer to stay in closely spaced planes. However, when $\Delta\gamma_1$ and $\Delta\gamma_2$ are very different and the NPs prefer to stay in planes well-separated from each other, they lead to the formation of bilayers. Experimentally, A_2B_3- and AB_3-type striped bilayers[23] have been obtained in binary systems of NPs and ABC_2-type bilayers[23] have been obtained in ternary systems (Figures 2d−f).

Computational modeling has played a key role in explaining the experimentally observed structures and discovering new ones. Although the idea of finding a particle arrangement that minimizes the free energy ΔF_N is straightforward, the optimization problem is challenging to solve. This is because many particles ($N \approx 30-100$) are needed to explore complex periodic structures with large unit cells, which increases the dimensionality ($3N$) of the configurational space. Recently, this problem was tackled using simplified pair potentials for interparticle interactions and an efficient global optimization approach, namely, a basin-hopping Monte Carlo method with particle "moves" tailored for interfacial systems.[19] This strategy enabled exhaustive exploration of the range of monolayer and bilayer superlattices achievable with binary NP systems of varying size ratios, interaction strengths, and fluid preferences (Figure 3). Several monolayer superlattices such as the AB-type intertwined square and AB_2-type triangular lattices

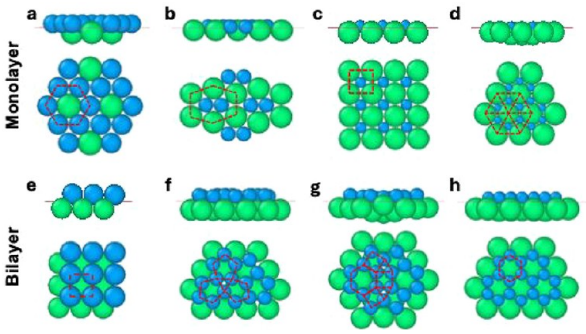

Figure 3. Binary superlattices of spherical NPs predicted by global Monte Carlo optimization. (a) AB_3-type lattice with Kagome-hexagonal ordering of NPs of size ratio $\varphi = 5/6$. (b) AB-type lattice with strained honeycomb order, $\varphi = 2/3$. (c) AB-type lattice with a square order at $\varphi = 1/2$. (d) AB_2-type lattice with triangular order at $\varphi = 1/3$. (e) AB-type lattice with square order at $\varphi = 1/2$. (f) A_3B_5-type lattice composed of slender pentagonal and triangular motifs at $\varphi = 2/3$. (g). A_4B_6-type lattice composed of hexagonal, square, and triangular motifs at $\varphi = 2/3$ (h) AB_2-type lattice with honeycomb order at $\varphi = 1/2$. [Panels are adapted with permission from ref 19. Copyright 2022, Springer Nature.]

realized experimentally with spherical NPs could be recovered,[2,25] as could structures assembled from disc- and rod-shaped NPs, such as AB- and AB_2-type lattices with stretched hexagonal and rhombic arrangement of particles.[26] The optimization also uncovered several structures that are yet to be experimentally realized; these include the AB_3-type monolayer (Figure 3a) and A_3B_5- and A_4B_6-type bilayer superlattices (Figures 3f and 3g). Interestingly, in many of the predicted bilayer superlattices, it is the smaller NP species that exhibits the unique arrangement, whereas the larger species due to its stronger interparticle interactions simply adopts a close-packed triangular lattice.

https://doi.org/10.1021/acs.langmuir.4c03321
Langmuir 2024, 40, 26800−26810

The full-scale 3D system with explicit distance-dependent interparticle interactions and interfacial energies considered in the above optimization can be simplified by projecting it onto a 2D plane and retaining only excluded-volume interactions between particles. The spherical particles are now reduced to hard discs that are allowed to partially overlap with each other when they belong to different species.[24,27] By evaluation of the closest-packed structures expected to form under infinite pressure conditions, such binary systems of partially overlapping hard disks could reproduce some of the lattices obtained with the detailed 3D model. This observation suggests that it may be possible to use maximum-packing ideas to rapidly discover plausible assembly morphologies, but relating the overlap parameter in the model to the physical parameters of the interfacial assembly system may be tedious, requiring a similar level of calculations used for predicting assembly morphologies in the 3D system.

Apart from periodic superlattices, interfacial assembly can be used to assemble aperiodic structures like quasicrystals (Figure 2c).[27,28] The formation of quasicrystals over periodic crystals may be rationalized by the larger number of degenerate patterns that can be obtained through random tiling as opposed to periodic tiling of particle motifs. Indeed, free-energy calculations show that the higher stability of dodecagonal quasicrystals arises predominantly from increase in configurational entropy rather than vibrational entropy.[29]

■ ANISOTROPIC NANOPARTICLES

Anisotropic NPs are appealing building blocks for material fabrication due to their ability to self-assemble into architectures unattainable by spherical NPs.[30,31] Given that anisotropic NPs individually exhibit intriguing anisotropic properties, such as preferred magnetization axes,[32] multiple surface plasmon resonance (SPR) modes,[33] and enhanced catalytic activity at specific facets,[34] their assemblies also often demonstrate unique collective properties. For instance, assemblies of Ag nanocubes with vertex or edge contacts between particles exhibit a blue shift in SPRs and a red shift in the case of assemblies with face−face contacts.[35]

Unlike spherical NPs, which only have translational degrees of freedom, anisotropic NPs also possess rotational degrees of freedom. Thus, when trapped at fluid−fluid interfaces, anisotropic NPs have the freedom to adjust not only their position z but also their orientation Ω in a way that minimizes the overall free energy ΔF_1 (Figure 4, top). As in the case of spherical NPs, ΔF_1 is given by the sum of the free energy gained from the particle occluding the interface and the free energy lost due to the particle contacting the less favored fluid. The occluded interfacial area and the particle−fluid contact area can be analytically expressed as a function of z and Ω for most regular particle geometries, leading to a function $\Delta F_1(z, \Omega)$ which can be minimized to obtain the equilibrium interfacial configuration of the NP denoted by z_{eq} and Ω_{eq}.[36] According to this model, anisotropic NPs such as prolate ellipsoids and nanocubes that interact equally favorably with the two fluids making up the interface should position themselves symmetrically at the interfacial plane and adopt horizontal (ellipsoids) or edge-up (nanocubes) orientations to occlude the largest possible interfacial area (as $\Delta\gamma = 0$).[36−38]

The above model assumes that the interface remains flat around the trapped NP.[36] However, the trapped NP could induce interface deformations due to contact angle constraints imposed by Young's law.[39,40] The impact of such deformations

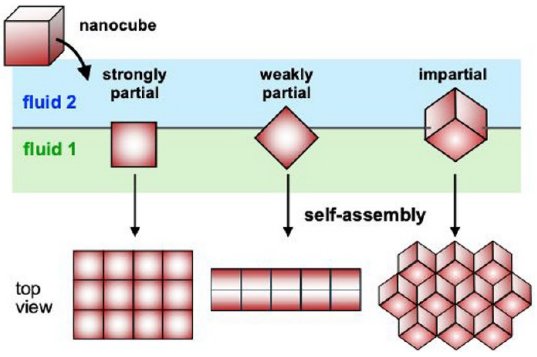

Figure 4. Tunable orientation and assembly of anisotropic NPs at fluid-fluid interfaces. Nanocubes strongly partial to one fluid lie face-up, promoting the assembly of square lattices with face−face contacts between NPs. Those weakly partial to one fluid lie edge-up and promote assembly of rods with face−face contacts, and those impartial to both fluids lie vertex-up and promote assembly of triangular lattices with edge−edge contacts.

on the equilibrium interfacial configuration of NPs can be determined by adding a capillary deformation term to ΔF_1 and then minimizing the resulting free-energy expression. When applied to nanocubes, the vertex-up orientation now becomes the globally stable state, in contrast to the edge-up orientation obtained when deformations are ignored.[40] This issue has also been investigated by molecular dynamics (MD) simulations using coarse-grained (CG) models.[37] With the ability to capture the true instantaneous shape of the interface and thereby quantify its true area occluded by particles, these simulations were able to confirm that the vertex-up orientation indeed occludes more interfacial area than the edge-up orientation. Another assumption commonly made in models is that the interface has zero thickness. However, this is strictly valid only for NPs much larger than the interfacial mixing region of the two fluids, which has a thickness on the order of a few nanometers.[41] For smaller NPs, the effect of nonzero thickness can be captured by replacing the interfacial area occlusion term in the free-energy model with an interfacial volume occlusion term. Interestingly, this correction can also explain the stabilization of the vertex-up orientation over the edge-up orientation for small nanocubes.[42,43]

The shape-asymmetry and orientation-dependent interactions inherent in anisotropic NPs lead to diverse modes of contact between NPs and unique assembly morphologies. Polyhedral NPs, for instance, can assemble through their faces, edges, or vertices (Figure 4, bottom). This is best illustrated using Ag nanocubes assembling at an oil−water interface.[44] The orientation of nanocubes can be tuned by varying the ratio of hydrophilic and hydrophobic molecules attached to their surface, which causes the NPs to self-assemble into distinct 2D superlattices: a square lattice of face-up nanocubes with face−face contacts; a linear string of edge-up nanocubes with face−face contacts; and a triangular lattice of vertex-up nanocubes with edge−edge contacts (Figures 5a−c). Other polyhedral NP shapes that have been assembled into 2D superlattices at a fluid interface include truncated cubes, cuboctahedra, and octahedra, with all polyhedral NPs forming close-packed lattices with face−face contacts between NPs.[45] These assemblies were obtained at an air−water interface using the Langmuir−Blodgett technique, which allows control over surface pressure of air−liquid film or effectively the density of trapped NPs at the interface.

https://doi.org/10.1021/acs.langmuir.4c03321
Langmuir 2024, 40, 26800−26810

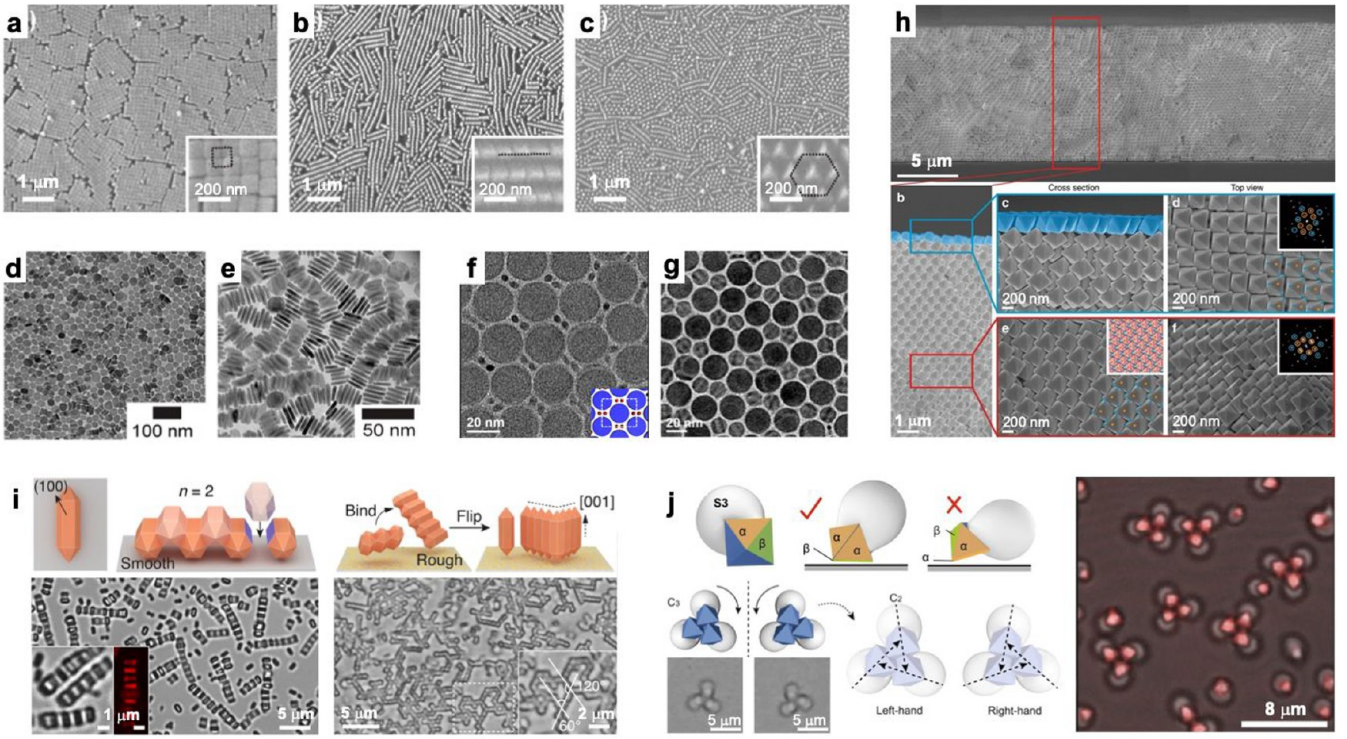

Figure 5. Self-assembly of anisotropic NPs into unique architectures at interfaces. (a–c) Ag nanocubes can form three distinct superlattices at an oil–water interface based on the ratio of hydrophobic–hydrophilic groups on their surface: square-arranged lattices with face-up nanocubes (a), linear structures with edge-up NPs (b), and hexagonal lattices with vertex-up NPs (c). (d, e) Cu_xS_y disks with hydrophilic and hydrophobic surface functionalization form hexagonal monolayer (d) and vertically oriented stacks (e) at an air–water interface. (f) Co-assembly of LaF_3 nanodisks and CdSe/CdS nanorods at air–water interface form an AB_2-type superlattice, while (g) coassembly of small and large LaF_3 nanodisks lead to an AB-type superlattice with stretched hexagon motifs. (h) Dual crystal structure assembled on a solid substrate from an evaporating droplet containing Ag octahedra, with the top and bulk layers possessing open and close-packed crystalline arrangement of NPs. (i) MOF-based hexagonal nanorods with pyramidal tips assemble into chains of horizontally oriented NPs on a smooth surface and snowflake-like structures with vertically oriented NPs on a rough surface. (j) Chiral trimers assembled from the assembly of octahedron-sphere hybrid Janus NPs promoted by the binding of the octahedra β–facet to a solid substrate. [Panels (a)–(c) have been adapted with permission from ref 44. Copyright 2016, American Chemical Society, Washington, DC. Panels (d) and (e) have been adapted with permission from ref 48. Copyright 2011, American Chemical Society, Washington, DC. Panels (f) and (g) have been adapted with permission from ref 26. Copyright 2015, American Chemical Society, Washington, DC. Panel (h) has been adapted with permission from ref 49. Available under a CC-BY 4.0 license. Copyright Lee et al. Panel (i) has been adapted with permission from ref 50. Available under a CC-BY 4.0 license. Copyright Lyu et al. Panel (j) has been adapted with permission from ref 51. Available under a CC-BY 4.0 license. Copyright 2015, Zhang et al.]

Researchers have also studied the interfacial assembly of other anisotropic NPs such as rods, ellipsoids, and disks. Rods and prolate ellipsoids, which tend to lie flat at the interface, self-assemble into 2D nematic or smectic liquid-crystalline phases depending on their aspect ratio.[46,47] Disk-shaped NPs can form two different types of assemblies at an air–water interface:[48] when the disks are hydrophobic, they stand vertically and form stacks to minimize their interaction with water, and when the disks are hydrophilic, they lay flat at the interface to maximize their interaction with water and form triangularly ordered monolayers (Figures 5d and 5e). More intricate assemblies can be achieved with mixtures of disks and/or rods. Binary mixtures of disks and thin rods organize into AB- and AB_2-type superlattices in which the disks lie flat at the interface and form square and rhombic sublattices while the rods stand vertically as monomers or dimers occupying the interstices of the disk sublattice (Figures 5f and 5g).[26] Interestingly, both these structures have been computationally predicted from binary systems of spherical NPs of similar size ratio.[19] Additionally, ternary systems of small and large disks and thin rods have been shown to self-assemble into an ABC-type superlattice.[26]

In some assembly scenarios, a solid substrate exists beneath the fluid–fluid interface, which can lead to interesting outcomes. First, in the case of drying NP-carrying droplets on a substrate, the evaporation process can lead to two distinct microenvironments: the drying front and the air–water interface. This leads to multilayered NP assemblies upon drying, where the top layer exhibits an organization of NPs different from the internal layers, which exhibit bulklike lattices, as demonstrated recently using polyhedral Ag nanocrystals (Figure 5h).[49] Second, the solid substrate can help tune the orientation and assembly architecture of anisotropic NPs: smooth surfaces that provide favorable surface-particle interactions promote assemblies with face-down orientation of NPs, even if they do not lead to maximum packing, whereas rough surfaces that are unable to provide sufficiently strong surface-particle interactions promote maximally packed NP assemblies with face-to-face contacts (Figure 5i). This strategy was recently applied to polyhedral metal–organic framework (MOF) particles, which were found to self-assemble into a range of superstructures, including 1D chains and 2D films,[50] and to Janus particles made of octahedral MOF

https://doi.org/10.1021/acs.langmuir.4c03321
Langmuir 2024, 40, 26800–26810

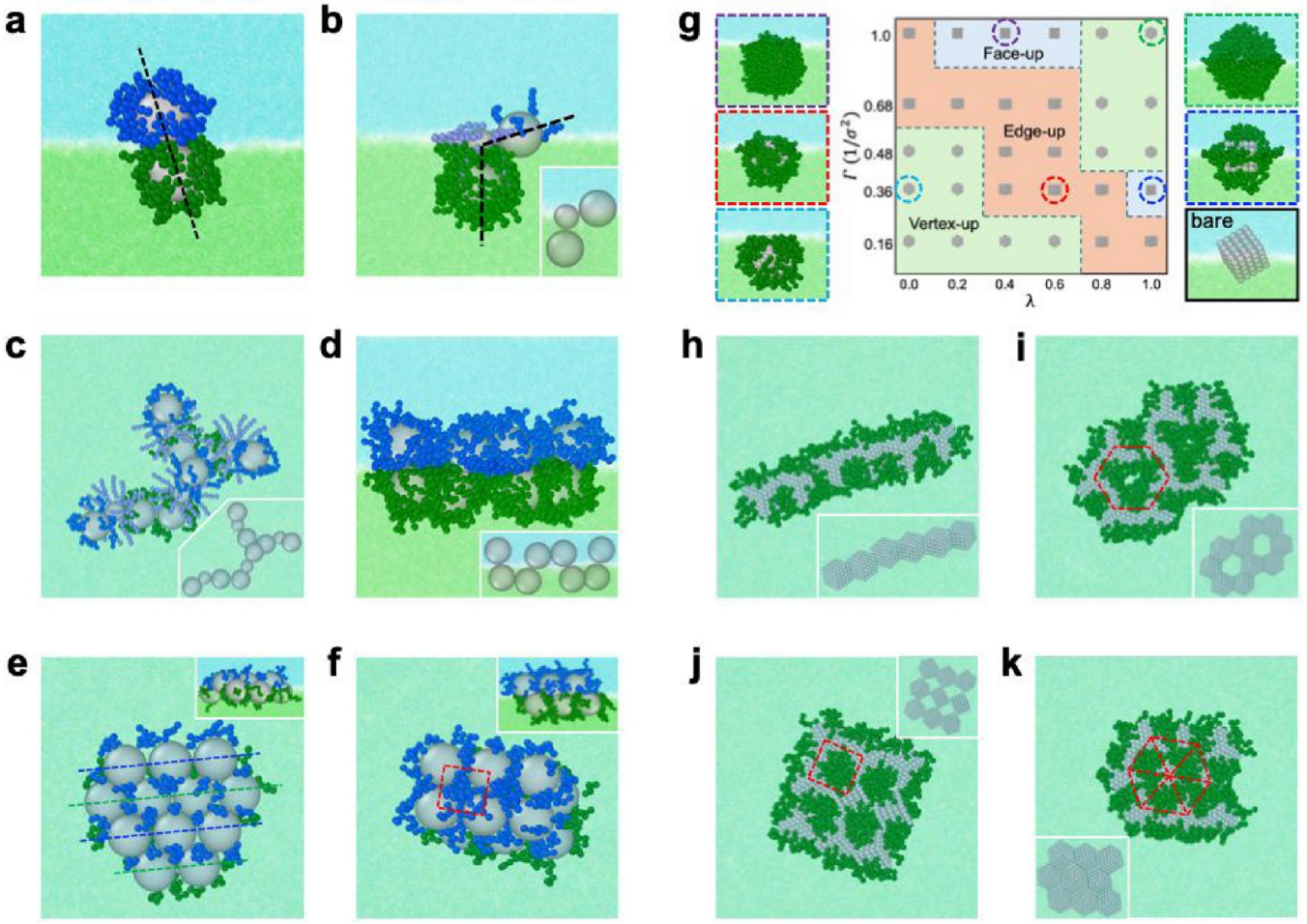

Figure 6. Tunable assembly of NPs into clusters, strings, networks, and superlattices through polymer grafting as predicted by MD simulations. (a–f) Interfacial assembly of spherical NPs into stable dimers with tunable tilt (panel (a)), stable trimers with tunable bending angle (panel (b)), tribranched networks (panel (c)), serpentine strings (panel (d)), ridged monolayers (panel (e)), and square bilayers (panel (f)). All assemblies were formed using two species of particles grafted with chains that favor opposite fluids of the interface, *except* the network shown in panel (c), which involved an additional species of particles smaller in size and grafted with chains impartial to both fluids. (g) Tuning the orientation of nanocubes with polymer grafts of different grafting density (Γ) and ratio of interaction strength with the two fluids (λ). Without grafts, the nanocubes exhibit vertex-up orientation as they are impartial to both fluids. (h–k) Self-assembly of nanocubes into edge–edge connected strings (panel (h)), edge–edge connected perforated hexagonal sheets (panel (i)), vertex–vertex-connected perforated square sheets (panel (j)), and edge–edge-connected triangular sheets (panel (k)). [Panels (a)–(f) have been adapted with permission from ref 18. Copyright 2019, American Chemical Society, Washington, DC. Panels (g)–(k) are adapted with permission from ref 37. Copyright 2022, American Chemical Society, Washington, DC.]

particles and solidified oil droplets, which assembled into chiral dimer and trimer clusters (Figure 5j).[51]

■ POLYMER-GRAFTED NANOPARTICLES

Polymer chains grafted onto NP surfaces can introduce steric repulsion and anisotropic attraction between NPs in the bulk, which can be harnessed for stabilizing NP dispersions[52] or directing NP assembly into low-dimensional architectures.[53,54] At fluid–fluid interfaces, polymer grafting can introduce additional, more-complex effects. Below we discuss how polymeric grafts can modify the surface chemistry of NPs and undergo conformational changes to influence the position and orientation of NPs at an interface and how they can introduce directional multibody interactions between NPs, all of which critically influence NP assembly at interfaces.

Polymer grafting, first and foremost, offers a versatile strategy for modulating the interaction of NPs with the interface. Polymer grafts are an excellent "knob" for manipulating the position of spherical NPs at the interface. The surface energy difference $\Delta\gamma$ which dictates the equilibrium distance z_{eq} of individual NPs from the interfacial plane can be tuned by adjusting the chemistry of the grafts and/or their grafting density.[18] MD simulations predict that two species of spherical NPs trapped on opposite sides of the interfacial plane via grafts favoring opposite fluid layers can coassemble into dimers, strings, monolayers, or bilayers by simply changing the grafting density (Figures 6a–f). Polymer grafts can also manipulate the orientation of anisotropic NPs trapped at the interface. Grafts with higher selectivity for one fluid over the other can push NPs farther away from the interfacial plane, thereby stabilizing orientations different from those a bare NP would prefer. Indeed, simulations predict that all three principal orientations of nanocubes (vertex-up, edge-up, and face-up) now become accessible by varying the grafting density and interaction preference of the grafts (Figure 6g).[37] The different orientations promote different types of contacts

https://doi.org/10.1021/acs.langmuir.4c03321
Langmuir 2024, 40, 26800–26810

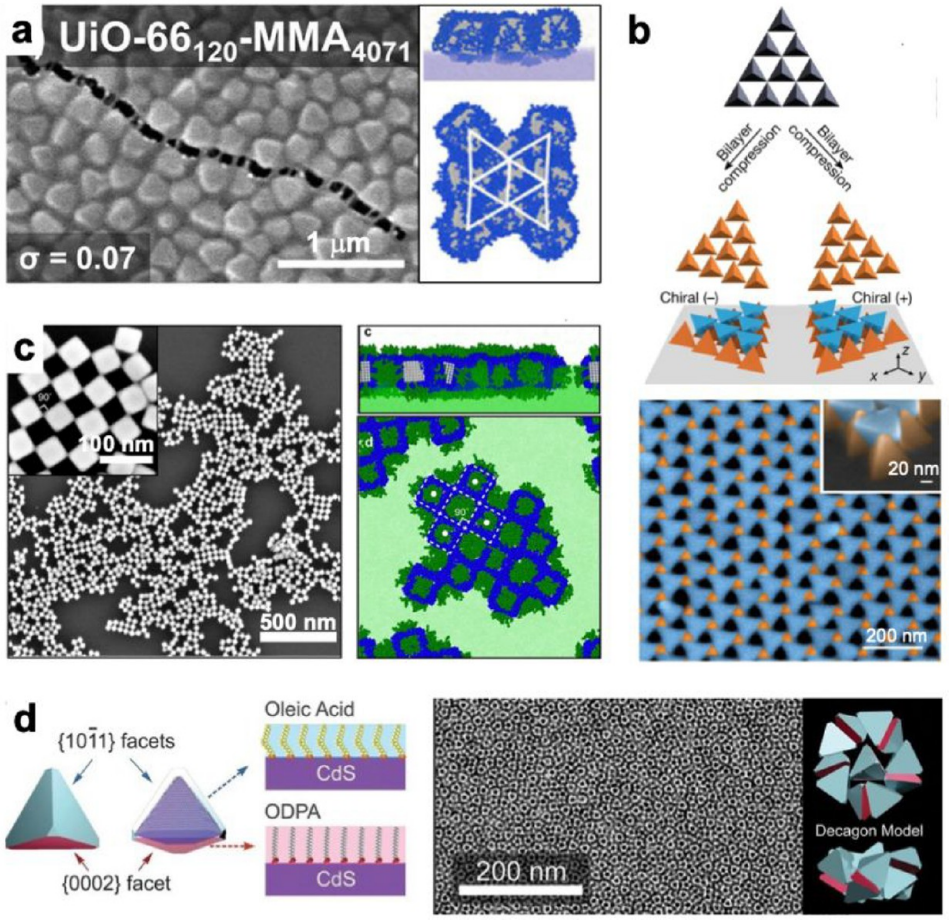

Figure 7. Polymer-mediated interactions between faceted NPs leads to novel assembly architectures at interfaces. (a) Hydrophobic interactions between polymer grafts on octahedral MOF NPs facilitate their assembly into robust free-standing films (left) whose assembly mechanism and architecture can be predicted well by MD simulations (right). (b) Repulsion of charged ligands on the surface of tetrahedral Au NPs leads to the assembly of chiral pinwheel superlattices. (c) Mixture of hydrophilic polymer chains and hydrophobic ligand grafts introduced onto the surface of Ag nanocubes enables their assembly into checkerboard lattices, demonstrated both experimentally (left) and in simulations (right). (d) Facet-dependent grafting of ligands to tetrahedral NPs leads to their assembly into quasicrystals. [Panel (a) has been adapted with permission from ref 58. Copyright 2022, American Chemical Society, Washington, DC. Panel (b) has been adapted with permission from ref 59. Copyright 2022, Springer Nature. Panel (c) has been adapted with permission from ref 60. Available under a CC-BY 4.0 license. Copyright Wang et al. Panel (d) has been adapted with permission from ref 61. Copyright 2018, AAAS.]

between NPs, leading to distinctive assemblies such as rectilinear strings, bilayer ribbons, perforated hexagonally ordered sheets with edge−edge contacts, and perforated square-ordered sheets with vertex−vertex contacts (Figures 6h−k).

As a result of their interaction with the interface, polymer grafts can undergo large conformational changes. These changes arise from the competition between chains, attempting to maximize their occlusion of the interface, minimize their interaction with the less-favored fluid, and maximize their conformational entropy. Simulations have provided significant insights into these conformational changes, revealing that the originally spherical corona of grafts around a uniformly grafted spherical NP adopts a lens-like shape at the interface due to chain stretching and intercalating into the interfacial mixing zone between the two fluids.[55,56] Such stretching behavior has also been confirmed experimentally using atomic force microscopy.[56] The extent of chain stretching at the interface can be predicted using a Flory-type model by minimizing the free energy of the grafts comprised of chain-fluid interaction energy, chain-stretching elastic energy, and chain−interface occlusion free energy.[57] Intriguingly, chain stretching can stabilize specific orientations of anisotropic NPs at the interface. For example, nanocubes grafted with chains that are impartial to both fluids, position themselves symmetrically at the interface and, intriguingly, adopt face-up orientation as it allows their grafts to maximally stretch out toward the interface, potentially leading to greater overall occlusion of the interface as compared to their nominal vertex-up orientation (Figure 6g).[37] Chain stretching can also impact the interfacial assembly of NPs by controlling the spacing between NPs in the assembled structures as a result of steric repulsion[56] and stabilizing the formation of NP clusters by preventing lateral assembly of NPs while allowing assembly normal to the interface (see Figures 6a and b).[18]

In addition to influencing NP−interface interactions, polymer grafts can alter the interactions between NPs. In the simplest scenario, solvophobic polymer chains are used for introducing robust attractive interactions between NPs that otherwise do not exhibit significant interactions. This approach was recently shown to lead to the formation of robust free-standing monolayers of octahedral MOF particles at an air−

https://doi.org/10.1021/acs.langmuir.4c03321
Langmuir 2024, 40, 26800−26810

water interface (Figure 7a).[58] In other cases, grafting is required to introduce repulsion between NPs that are otherwise strongly attractive. For instance, attaching charged chains to NPs can introduce electrostatic repulsion, making face-to-face contacts less favorable than other contacts that involve smaller overlap between NP surfaces. This strategy was used for promoting corner−edge contacts between tetrahedral gold NPs, enabling the formation of chiral pinwheel superlattices on a solid substrate (Figure 7b).[59] Sometimes, multiple types of grafts are needed to achieve superlattices with a specific NP-NP contact and NP orientation. This is best exemplified by the assembly of checkerboard lattices of Ag nanocubes at an air−water interface, where the edge−edge contacts and face-up orientation of nanocubes necessary for forming the structure were enabled by grafting a mixture of short hydrophobic ligands and long hydrophilic chains to the nanocubes (Figure 7c).[60] The balance of hydrophobic and hydrophilic interactions led to face-up orientation of nanocubes, the hydrophobic ligands provided the necessary interparticle attraction to drive self-assembly, and the hydrophilic chains provided the steric repulsion to promote edge−edge contacts over face−face contacts. Complex assemblies at the interface can also be realized through "patchy" grafting of NPs. For instance, tetrahedral NPs grafted with one ligand on three facets and another on the remaining facet were shown to self-assemble into quasicrystals at an air−liquid interface (Figure 7d).[61]

Lastly, long polymer grafts can introduce many-body effects, leading to emergent anisotropic assemblies. In the bulk, spherical NPs with homogeneously grafted chains can self-assemble into 1D strings, 2D sheets, and 3D globular structures. Since the effective two-body (pairwise) interactions between such NPs are isotropic, they can only account for the formation of the 3D assemblies but not the 1D and 2D assemblies. The emergence of these structures has been attributed to higher-body interactions.[62] Specifically, due to the deformable nature of polymer chains, the conformation of grafts between two or more interacting NPs is perturbed by the insertion of grafts from another proximal NP, leading to a net interaction different from that obtained by simply summing up the interactions between all pairs of particles.[63] For instance, when two NPs form a dimer, the grafts are expelled from the region between them due to the excluded volume of the NP cores. Consequently, the graft segment density around the contact region of the dimer increases compared to its poles, causing a third approaching NP to experience a steric repulsion that is stronger than the sum of the repulsions from the two particles of the dimer in isolation. These same many-body effects can also influence the interfacial assembly of polymer-grafted NPs, leading to quasi-1D structures like serpentine strings and tribranched networks (Figures 6c and 6d).[18] These interactions combined with effects from the interface prevent NPs from forming multiple contacts necessary to achieve 2D structures, favoring instead one or two contacts that lead to strings and branched networks. Explicitly capturing many-body effects in assembly simulations is computationally expensive, but recent advances in machine learning (ML) have shown promise. ML methods can derive "effective" potentials to efficiently capture the complex many-body interactions between polymer-grafted NPs by appropriately integrating out the polymeric degrees of freedom.[64,65] Such potentials have been shown to accurately reproduce known phases in 3D polymer−nanoparticle systems, such as 1D strings and 2D hexagonal sheets, and to predict new structures such as networks, clusters, and gels.[65]

OUTLOOK

We have discussed how ligand-grafted spherical and anisotropic NPs can self-assemble into a rich variety of low-dimensional structures, such as clusters, strings, networks, superlattices, chiral lattices, and quasicrystals, at fluid−fluid interfaces. While the past decade has witnessed enormous progress in the field of interfacial assembly, several theoretical and experimental challenges will need to be resolved over the next decade to drive further development in this exciting field.

Compared to the behavior of polymer-grafted spherical NPs and bare anisotropic NPs at fluid−fluid interfaces,[18,42] our understanding of the interaction of polymer-grafted anisotropic NPs with interfaces is less developed. This is due to the combined complexity of polymer deformation at the interface and interfacial deformation induced by the NP. Developing a theoretical model that can accurately predict the interfacial behavior of such particles is highly desirable. The model should be able to not only account for the conformation of polymer chains at an interface and the deformation of an interface by the NP, but also quantify the free energy changes associated with these changes in polymer-fluid and fluid−fluid interactions. Even more desirable will be treatment of two or more NPs trapped at the interface, as the net interfacial deformation and change in polymer conformation will likely not be a simple superposition of the effects of individual NPs. At the same time, it would be useful to experimentally characterize the conformation of NP-attached polymer chains at the interface.[66]

Many-body interactions between polymer-grafted NPs are responsible for their assembly into quasi-1D structures at interfaces.[18] The full potential of such interactions in producing unique assembly architectures, however, remains underexplored. While effective potentials capable of capturing many-body interactions between polymer-grafted spherical NPs in bulk solvent have been developed using ML methods,[65] creating similar effective potentials for NPs residing at interfaces presents challenges. The potential will have to be described in terms of additional coordinates, such as the distance of NPs from the interfacial plane, and the impact of polymer deformation at the interface on NP−NP interactions will also need to be considered. Once developed, such a potential could be coupled with existing free energy models of NP−interface interactions and used in MD simulations to rapidly explore the scope of anisotropic assemblies achievable at interfaces. Similar ML approaches could be used for deriving many-body potentials for anisotropic NPs—where many-body effects may be even more prominent—and for systems containing multiple species of NPs. In the former case, additional angular parameters will be needed to describe the relative orientation of NPs, and in the latter case, species-specific interparticle distances will need to be considered.

Global optimization algorithms have shown enormous promise for discovering 2D superlattices formed at interfaces from binary systems of NPs of different sizes.[19] However, the free energy model used in these algorithms considers the interaction strength between unlike NPs to be intermediate to that between like NPs. Therefore, it would be worthwhile to explore a broader range of interaction strengths, which could help uncover additional superlattice architectures that may be attainable at interfaces. The optimization approach could also

https://doi.org/10.1021/acs.langmuir.4c03321
Langmuir 2024, 40, 26800−26810

be readily extended to predict ternary or quaternary superlattices by incorporating additional NP species of distinct sizes or surface chemistries, a prospect too challenging to explore purely experimentally. Furthermore, the approach could be combined with many-body potentials to reveal more irregular and anisotropic NP assemblies formed at interfaces. Lastly, the free-energy models could be further improved by including entropy contributions, such as configurational entropy that is known to stabilize the formation of quasicrystals.[29] This could facilitate the discovery of quasicrystal or chiral superlattices self-assembled at interfaces.

As compared to spherical NPs, much less effort has been devoted to studying the interfacial assembly of single-component and multicomponent systems of anisotropic NPs. Anisotropic NPs, especially those with faceted geometries, have the potential to form complex assembly architectures. Take for instance chiral superlattices and quasicrystals assembled from tetrahedral NPs[59,61] or checkerboards assembled from nanocubes at liquid interfaces.[60] However, the multiple ways in which faceted NPs can bind to each other can strongly reduce the yield of the targeted assembly by trapping the assembly domains with "wrong" NP-NP contacts. Current droplet evaporation, film compression, and thermal annealing strategies for self-assembling NPs will thus have to be refined to improve the assembly yields.

The driving forces for NP assembly could be further developed to achieve more complex and fascinating structures. For example, incorporating patchy interactions between NPs through nonuniform grafting of ligands onto NP facets can lead to novel assembly behaviors.[60,61] Specific complementary interactions could be engineered into the NPs by grafting chains featuring dynamic hydrogen bonds, oppositely charged moieties, or DNA strands.[67−69] NPs with such specifically designed interactions have a higher chance of assembling into intricate NP architectures in high yield. Additionally, interactions could be further tuned by using external fields such as magnetic, electrical, or acoustic fields. For instance, magnetic Janus particles have shown the ability to form reconfigurable hexagonal lattices on spherical droplet interfaces, which can be precisely controlled by altering the direction of the magnetic field.[70] The interplay between interfacial and external forces could open exciting opportunities for creating unique, tunable, and reconfigurable assemblies.

Finally, more experimental work is needed to validate the many new computationally predicted NP assembly structures. The stable dimers with tunable tilt angles and trimers with tunable bending angle predicted to form at interfaces with strongly grafted NPs (Figure 6a, b),[18] the 2D binary NP superlattices with pentagonal and multishape tessellation arrangements (see Figures 3f and 3g),[19] and the 2D quasicrystals predicted to form from mixtures of small and hard spheres on a flat plane[29] are all highly promising candidates for future experimental investigations. Furthermore, exploring the unique properties and potential applications of these discovered NP structures would be a highly fruitful venture.

AUTHOR INFORMATION

Corresponding Author

Gaurav Arya − *Department of Mechanical Engineering and Materials Science, Duke University, Durham, North Carolina 27708, United States;* orcid.org/0000-0002-5615-0521; Phone: +1 (919) 660-5435; Email: gaurav.arya@duke.edu; Fax: +1 (919) 660-8963

Authors

Yilong Zhou − *Materials Science Division, Lawrence Livermore National Laboratory, Livermore, California 94550, United States*

Şafak Çallıoğlu − *Department of Mechanical Engineering and Materials Science, Duke University, Durham, North Carolina 27708, United States;* orcid.org/0000-0002-7491-2497

Complete contact information is available at: https://pubs.acs.org/10.1021/acs.langmuir.4c03321

Notes

The authors declare no competing financial interest.

Biographies

Yilong Zhou is a postdoctoral researcher in the Lawrence Livermore National Laboratory, USA. He received his B.S. in Naval Architecture and Ocean Engineering from Huazhong University of Science and Technology, China in 2013, M.S. in Mechanical Engineering from Clemson University, USA in 2016, and Ph.D. in Mechanical Engineering and Materials Science from Duke University, USA in 2022. His research interests are in ab initio, molecular simulation, and finite elements modeling of nanoparticle assembly, fluid flow, and ion transport.

Şafak Çallıoğlu is a Ph.D. student in the Department of Mechanical Engineering and Materials Science at Duke University, USA. He obtained B.S. degree in Physics as well as Electrical and Electronics Engineering from Bilkent University, Turkey in 2022. His current research focuses on the use of molecular simulations and machine learning to control nanoparticle assembly at interfaces.

https://doi.org/10.1021/acs.langmuir.4c03321
Langmuir 2024, 40, 26800−26810

Gaurav Arya is a Professor in the Department of Mechanical Engineering and Materials Science at Duke University, USA. He received his B. Tech. from Indian Institute of Technology Bombay, India in 1998 and his Ph.D. from University of Notre Dame, USA in 2003, both in chemical engineering. He carried out postdoctoral research at Princeton University and New York University. His research group uses molecular simulations, statistical mechanics, and machine learning to predict and gain molecular-level understanding of material properties, with the overarching aim of discovering new phenomena and developing new materials. His current research falls within the themes of polymer−nanoparticle composites, DNA nanotechnology, and DNA translocation motors.

■ ACKNOWLEDGMENTS

The authors would like to thank the National Science Foundation-funded UC San Diego Materials Research Science and Engineering Center (Grant No. DMR-2011924) for financial support. Portion of this work was performed under the auspices of the Department of Energy by Lawrence Livermore National Laboratory (Contract No. DE-AC52-07NA27344).

■ REFERENCES

(1) Nie, Z.; Petukhova, A.; Kumacheva, E. Properties and emerging applications of self-assembled structures made from inorganic nanoparticles. *Nature Nanotechnol.* **2010**, *5* (1), 15−25.
(2) Kang, Y.; Ye, X.; Chen, J.; Qi, L.; Diaz, R. E.; Doan-Nguyen, V.; Xing, G.; Kagan, C. R.; Li, J.; Gorte, R. J.; Stach, E. A.; Murray, C. B. Engineering catalytic contacts and thermal stability: gold/iron oxide binary nanocrystal superlattices for CO oxidation. *J. Am. Chem. Soc.* **2013**, *135* (4), 1499−1505.
(3) Kumar, S. K.; Jouault, N.; Benicewicz, B.; Neely, T. Nanocomposites with polymer grafted nanoparticles. *Macromolecules* **2013**, *46* (9), 3199−3214.
(4) Dong, A.; Chen, J.; Vora, P. M.; Kikkawa, J. M.; Murray, C. B. Binary nanocrystal superlattice membranes self-assembled at the liquid-air interface. *Nature* **2010**, *466* (7305), 474−477.
(5) Yao, C.; Yan, W.; Dong, R.; Dou, S.; Yang, L. Superlattice assembly strategy of small noble metal nanoparticles for surface-enhanced Raman scattering. *Commun. Mater.* **2024**, *5* (1), 65.
(6) Kim, K.; Sherman, Z. M.; Cleri, A.; Chang, W. J.; Maria, J.-P.; Truskett, T. M.; Milliron, D. J. Hierarchically doped plasmonic nanocrystal metamaterials. *Nano Lett.* **2023**, *23* (16), 7633−7641.
(7) Lotito, V.; Zambelli, T. Self-assembly of single-sized and binary colloidal particles at air/water interface by surface confinement and water discharge. *Langmuir* **2016**, *32* (37), 9582−9590.
(8) Guzmán, E.; Maestro, A. Soft colloidal particles at fluid interfaces. *Polymers* **2022**, *14* (6), 1133.
(9) Ciarella, S.; Rey, M.; Harrer, J.; Holstein, N.; Ickler, M.; Lowen, H.; Vogel, N.; Janssen, L. M. Soft particles at liquid interfaces: From molecular particle architecture to collective phase behavior. *Langmuir* **2021**, *37* (17), 5364−5375.
(10) Deshmukh, O. S.; van den Ende, D.; Stuart, M. C.; Mugele, F.; Duits, M. H. Hard and soft colloids at fluid interfaces: Adsorption, interactions, assembly & rheology. *Adv. Colloid Interface Sci.* **2015**, *222*, 215−227.
(11) Feller, D.; Karg, M. Fluid interface-assisted assembly of soft microgels: recent developments for structures beyond hexagonal packing. *Soft Matter* **2022**, *18* (34), 6301−6312.
(12) Kralchevsky, P. A.; Nagayama, K. Capillary forces between colloidal particles. *Langmuir* **1994**, *10* (1), 23−36.
(13) Flatté, M.; Kornyshev, A.; Urbakh, M. Understanding voltage-induced localization of nanoparticles at a liquid-liquid interface. *J. Phys.: Condens. Matter* **2008**, *20* (7), 073102.
(14) Bresme, F.; Oettel, M. Nanoparticles at fluid interfaces. *J. Phys.: Condens. Matter* **2007**, *19* (41), 413101.
(15) Botto, L.; Lewandowski, E. P.; Cavallaro, M.; Stebe, K. J. Capillary interactions between anisotropic particles. *Soft Matter* **2012**, *8* (39), 9957−9971.
(16) Lehle, H.; Noruzifar, E.; Oettel, M. Ellipsoidal particles at fluid interfaces. *Eur. Phys. J. E* **2008**, *26*, 151−160.
(17) Davies, G. B.; Krüger, T.; Coveney, P. V.; Harting, J.; Bresme, F. Capillary Interactions: Assembling Ellipsoidal Particles at Fluid Interfaces Using Switchable Dipolar Capillary Interactions (Adv. Mater. 39/2014). *Adv. Mater.* **2014**, *26* (39), 6800.
(18) Tang, T. Y.; Zhou, Y.; Arya, G. Interfacial Assembly of Tunable Anisotropic Nanoparticle Architectures. *ACS Nano* **2019**, *13* (4), 4111−4123.
(19) Zhou, Y.; Arya, G. Discovery of two-dimensional binary nanoparticle superlattices using global Monte Carlo optimization. *Nat. Commun.* **2022**, *13* (1), 7976.
(20) Pieranski, P. Two-dimensional interfacial colloidal crystals. *Phys. Rev. Lett.* **1980**, *45* (7), 569.
(21) Law, B. M.; McBride, S. P.; Wang, J. Y.; Wi, H. S.; Paneru, G.; Betelu, S.; Ushijima, B.; Takata, Y.; Flanders, B.; Bresme, F.; et al. Line tension and its influence on droplets and particles at surfaces. *Progress Surface Sci.* **2017**, *92* (1), 1−39.
(22) Kuk, K.; Abgarjan, V.; Gregel, L.; Zhou, Y.; Carrasco Fadanelli, V.; Buttinoni, I.; Karg, M. Compression of colloidal monolayers at liquid interfaces: in situ vs. ex situ investigation. *Soft Matter* **2023**, *19* (2), 175−188.
(23) Dong, A.; Ye, X.; Chen, J.; Murray, C. B. Two-dimensional binary and ternary nanocrystal superlattices: the case of monolayers and bilayers. *Nano Lett.* **2011**, *11* (4), 1804−9.
(24) Raybin, J. G.; Wai, R. B.; Ginsberg, N. S. Nonadditive Interactions Unlock Small-Particle Mobility in Binary Colloidal Monolayers. *ACS Nano* **2023**, *17* (9), 8303−8314.
(25) Kim, H. J.; Wang, W.; Zhang, H.; Freychet, G.; Ocko, B. M.; Travesset, A.; Mallapragada, S. K.; Vaknin, D. Binary superlattices of gold nanoparticles in two dimensions. *J. Phys. Chem. Lett.* **2022**, *13* (15), 3424−3430.
(26) Paik, T.; Diroll, B. T.; Kagan, C. R.; Murray, C. B. Binary and ternary superlattices self-assembled from colloidal nanodisks and nanorods. *J. Am. Chem. Soc.* **2015**, *137* (20), 6662−9.
(27) Fayen, E.; Imperor-Clerc, M.; Filion, L.; Foffi, G.; Smallenburg, F. Self-assembly of dodecagonal and octagonal quasicrystals in hard spheres on a plane. *Soft Matter* **2023**, *19* (14), 2654−2663.
(28) Talapin, D. V.; Shevchenko, E. V.; Bodnarchuk, M. I.; Ye, X.; Chen, J.; Murray, C. B. Quasicrystalline order in self-assembled binary nanoparticle superlattices. *Nature* **2009**, *461* (7266), 964−7.
(29) Fayen, E.; Filion, L.; Foffi, G.; Smallenburg, F. Quasicrystal of Binary Hard Spheres on a Plane Stabilized by Configurational Entropy. *Phys. Rev. Lett.* **2024**, *132* (4), 048202.
(30) Damasceno, P. F.; Engel, M.; Glotzer, S. C. Predictive self-assembly of polyhedra into complex structures. *Science* **2012**, *337* (6093), 453−457.
(31) Sacanna, S.; Korpics, M.; Rodriguez, K.; Colón-Meléndez, L.; Kim, S.-H.; Pine, D. J.; Yi, G.-R. Shaping colloids for self-assembly. *Nat. Commun.* **2013**, *4* (1), 1688.

https://doi.org/10.1021/acs.langmuir.4c03321
Langmuir 2024, 40, 26800−26810

(32) Kronast, F.; Friedenberger, N.; Ollefs, K.; Gliga, S.; Tati-Bismaths, L.; Thies, R.; Ney, A.; Weber, R.; Hassel, C.; Römer, F. M.; et al. Element-specific magnetic hysteresis of individual 18 nm Fe nanocubes. *Nano Lett.* **2011**, *11* (4), 1710−1715.
(33) da Silva, A. G.; Rodrigues, T. S.; Wang, J.; Yamada, L. K.; Alves, T. V.; Ornellas, F. R.; Ando, R. A.; Camargo, P. H. The fault in their shapes: investigating the surface-plasmon-resonance-mediated catalytic activities of silver quasi-spheres, cubes, triangular prisms, and wires. *Langmuir* **2015**, *31* (37), 10272−10278.
(34) Deori, K.; Gupta, D.; Saha, B.; Deka, S. Design of 3-dimensionally self-assembled CeO_2 nanocube as a breakthrough catalyst for efficient alkylarene oxidation in water. *ACS Catal.* **2014**, *4* (9), 3169−3179.
(35) Yoon, J. H.; Selbach, F.; Schumacher, L.; Jose, J.; Schlücker, S. Surface plasmon coupling in dimers of gold nanoparticles: Experiment and theory for ideal (spherical) and nonideal (faceted) building blocks. *ACS Photonics* **2019**, *6* (3), 642−648.
(36) Shi, W.; Zhang, Z.; Li, S. Quantitative Prediction of Position and Orientation for Platonic Nanoparticles at Liquid/Liquid Interfaces. *J. Phys. Chem. Lett.* **2018**, *9* (2), 373−382.
(37) Zhou, Y.; Tang, T. Y.; Lee, B. H.; Arya, G. Tunable Orientation and Assembly of Polymer-Grafted Nanocubes at Fluid-Fluid Interfaces. *ACS Nano* **2022**, *16* (5), 7457−7470.
(38) Coertjens, S.; De Dier, R.; Moldenaers, P.; Isa, L.; Vermant, J. Adsorption of ellipsoidal particles at liquid-liquid interfaces. *Langmuir* **2017**, *33* (11), 2689−2697.
(39) Coertjens, S.; Moldenaers, P.; Vermant, J.; Isa, L. Contact angles of microellipsoids at fluid interfaces. *Langmuir* **2014**, *30* (15), 4289−4300.
(40) Soligno, G.; Dijkstra, M.; van Roij, R. Self-Assembly of Cubes into 2D Hexagonal and Honeycomb Lattices by Hexapolar Capillary Interactions. *Phys. Rev. Lett.* **2016**, *116* (25), 258001.
(41) Das, A.; Ali, S. M. Understanding of interfacial tension and interface thickness of liquid/liquid interface at a finite concentration of alkyl phosphate by molecular dynamics simulation. *J. Mol. Liq.* **2019**, *277*, 217−232.
(42) Gupta, U.; Hanrath, T.; Escobedo, F. A. Modeling the orientational and positional behavior of polyhedral nanoparticles at fluid-fluid interfaces. *Phys. Rev. Mater.* **2017**, *1* (5 055602.
(43) Gupta, U.; Escobedo, F. A. An Implicit-Solvent Model for the Interfacial Configuration of Colloidal Nanoparticles and Application to the Self-Assembly of Truncated Cubes. *J. Chem. Theory Comput.* **2020**, *16* (9), 5866−5875.
(44) Yang, Y.; Lee, Y. H.; Phang, I. Y.; Jiang, R.; Sim, H. Y.; Wang, J.; Ling, X. Y. A Chemical Approach To Break the Planar Configuration of Ag Nanocubes into Tunable Two-Dimensional Metasurfaces. *Nano Lett.* **2016**, *16* (6), 3872−8.
(45) Tao, A.; Sinsermsuksakul, P.; Yang, P. Tunable plasmonic lattices of silver nanocrystals. *Nat. Nanotechnol.* **2007**, *2* (7), 435−40.
(46) Dugyala, V. R.; Anjali, T. G.; Upendar, S.; Mani, E.; Basavaraj, M. G. Nano ellipsoids at the fluid-fluid interface: effect of surface charge on adsorption, buckling and emulsification. *Faraday Discuss.* **2016**, *186*, 419−434.
(47) Luo, A. M.; Vermant, J.; Ilg, P.; Zhang, Z.; Sagis, L. M. Self-assembly of ellipsoidal particles at fluid-fluid interfaces with an empirical pair potential. *J. Colloid Interface Sci.* **2019**, *534*, 205−214.
(48) Hsu, S.-W.; On, K.; Tao, A. R. Localized surface plasmon resonances of anisotropic semiconductor nanocrystals. *J. Am. Chem. Soc.* **2011**, *133* (47), 19072−19075.
(49) Lee, Y. H.; Lay, C. L.; Shi, W.; Lee, H. K.; Yang, Y.; Li, S.; Ling, X. Y. Creating two self-assembly micro-environments to achieve supercrystals with dual structures using polyhedral nanoparticles. *Nat. Commun.* **2018**, *9* (1), 2769.
(50) Lyu, D.; Xu, W.; Payong, J. E. L.; Zhang, T.; Wang, Y. Low-dimensional assemblies of metal-organic framework particles and mutually coordinated anisotropy. *Nat. Commun.* **2022**, *13* (1), 3980.
(51) Zhang, T.; Lyu, D.; Xu, W.; Feng, X.; Ni, R.; Wang, Y. Janus particles with tunable patch symmetry and their assembly into chiral colloidal clusters. *Nat. Commun.* **2023**, *14* (1), 8494.
(52) Krishnamoorti, R. Strategies for dispersing nanoparticles in polymers. *MRS Bull.* **2007**, *32* (4), 341−347.
(53) Yi, C.; Yang, Y.; Liu, B.; He, J.; Nie, Z. Polymer-guided assembly of inorganic nanoparticles. *Chem. Soc. Rev.* **2020**, *49* (2), 465−508.
(54) Hsu, S.-W.; Rodarte, A. L.; Som, M.; Arya, G.; Tao, A. R. Colloidal plasmonic nanocomposites: from fabrication to optical function. *Chem. Rev.* **2018**, *118* (6), 3100−3120.
(55) Schwenke, K.; Isa, L.; Cheung, D. L.; Del Gado, E. Conformations and effective interactions of polymer-coated nanoparticles at liquid interfaces. *Langmuir* **2014**, *30* (42), 12578−86.
(56) Vialetto, J.; Camerin, F.; Ramakrishna, S. N.; Zaccarelli, E.; Isa, L. Exploring the 3D Conformation of Hard-Core Soft-Shell Particles Adsorbed at a Fluid Interface. *Adv. Sci. (Weinh.)* **2023**, *10* (28), No. e2303404.
(57) Vasudevan, S. A.; Rauh, A.; Kroger, M.; Karg, M.; Isa, L. Dynamics and Wetting Behavior of Core-Shell Soft Particles at a Fluid-Fluid Interface. *Langmuir* **2018**, *34* (50), 15370−15382.
(58) Barcus, K.; Lin, P. A.; Zhou, Y.; Arya, G.; Cohen, S. M. Influence of Polymer Characteristics on the Self-Assembly of Polymer-Grafted Metal-Organic Framework Particles. *ACS Nano* **2022**, *16* (11), 18168−18177.
(59) Zhou, S.; Li, J.; Lu, J.; Liu, H.; Kim, J. Y.; Kim, A.; Yao, L.; Liu, C.; Qian, C.; Hood, Z. D.; Lin, X.; Chen, W.; Gage, T. E.; Arslan, I.; Travesset, A.; Sun, K.; Kotov, N. A.; Chen, Q. Chiral assemblies of pinwheel superlattices on substrates. *Nature* **2022**, *612* (7939), 259−265.
(60) Wang, Y.; Zhou, Y.; Yang, Q.; Basak, R.; Xie, Y.; Le, D.; Fuqua, A. D.; Shipley, W.; Yam, Z.; Frano, A.; Arya, G.; Tao, A. R. Self-assembly of nanocrystal checkerboard patterns via non-specific interactions. *Nat. Commun.* **2024**, *15* (1), 3913.
(61) Nagaoka, Y.; Zhu, H.; Eggert, D.; Chen, O. Single-component quasicrystalline nanocrystal superlattices through flexible polygon tiling rule. *Science* **2018**, *362* (6421), 1396−1400.
(62) Akcora, P.; Liu, H.; Kumar, S. K.; Moll, J.; Li, Y.; Benicewicz, B. C.; Schadler, L. S.; Acehan, D.; Panagiotopoulos, A. Z.; Pryamitsyn, V.; et al. Anisotropic self-assembly of spherical polymer-grafted nanoparticles. *Nat. Mater.* **2009**, *8* (4), 354−359.
(63) Tang, T.-Y.; Arya, G. Anisotropic three-particle interactions between spherical polymer-grafted nanoparticles in a polymer matrix. *Macromolecules* **2017**, *50* (3), 1167−1183.
(64) Giunta, G.; Campos-Villalobos, G.; Dijkstra, M. Coarse-Grained Many-Body Potentials of Ligand-Stabilized Nanoparticles from Machine-Learned Mean Forces. *ACS Nano* **2023**, *17* (23), 23391−23404.
(65) Zhou, Y.; Bore, S. L.; Tao, A. R.; Paesani, F.; Arya, G. Many-body potential for simulating the self-assembly of polymer-grafted nanoparticles in a polymer matrix. *npj Comput. Mater.* **2023**, *9*, 224.
(66) Besford, Q. A.; Uhlmann, P.; Fery, A. Spatially Resolving Polymer Brush Conformation: Opportunities Ahead. *Macromol. Chem. Phys.* **2023**, *224* (1), 2200180.
(67) Bian, T.; Gardin, A.; Gemen, J.; Houben, L.; Perego, C.; Lee, B.; Elad, N.; Chu, Z.; Pavan, G. M.; Klajn, R. Electrostatic co-assembly of nanoparticles with oppositely charged small molecules into static and dynamic superstructures. *Nat. Chem.* **2021**, *13* (10), 940−949.
(68) Rogers, W. B.; Shih, W. M.; Manoharan, V. N. Using DNA to program the self-assembly of colloidal nanoparticles and microparticles. *Nat. Rev. Mater.* **2016**, *1* (3), 1−14.
(69) Zhang, J.; Santos, P. J.; Gabrys, P. A.; Lee, S.; Liu, C.; Macfarlane, R. J. Self-assembling nanocomposite tectons. *J. Am. Chem. Soc.* **2016**, *138* (50), 16228−16231.
(70) Xie, Q.; Davies, G. B.; Harting, J. Direct Assembly of Magnetic Janus Particles at a Droplet Interface. *ACS Nano* **2017**, *11* (11), 11232−11239.

https://doi.org/10.1021/acs.langmuir.4c03321
Langmuir 2024, 40, 26800−26810